

Spin qubits in double quantum dots: Entanglement versus the Kondo effect

A. Ramšak,^{1,2} J. Mravlje,² R. Žitko,² and J. Bonča^{1,2}

¹Faculty of Mathematics and Physics, University of Ljubljana, Ljubljana, Slovenia

²J. Stefan Institute, Ljubljana, Slovenia

(Received 8 November 2006; published 21 December 2006)

We investigate the competition between pair entanglement of two spin qubits in double quantum dots attached to leads with various topologies and the separate entanglement of each spin with nearby electrodes. Universal behavior of entanglement is demonstrated in dependence on the mutual interactions between the spin qubits, the coupling to their environment, temperature, and magnetic field. As a consequence of quantum phase transition an abrupt switch between fully entangled and unentangled states takes place when the dots are coupled in parallel.

DOI: 10.1103/PhysRevB.74.241305

PACS number(s): 73.63.Kv, 03.67.Mn, 72.15.Qm

Introduction. After the recent discovery of quantum computing algorithms, their practical potential led to an interest in quantum entanglement spurred on by the fact that if a quantum computer were built, it would be capable of tasks impracticable in classical computing.¹ Nanostructures consisting of coupled quantum dots are candidates for the required scalable solid-state arrays of electron spin qubits.^{2,3} The interaction of such qubits with the environment is in general a complicated many-body process, and its understanding is crucial for experimental solid-state realization of qubits in single and double quantum dots (DQD's).⁴ Recent experiments on semiconductor double-quantum-dot devices have shown that electron occupation may be controlled down to the single-electron level by surface gates.⁵ Also spin-entangled states were detected,⁶ DQD's were used to implement two-electron spin entanglement,⁷ and coherent manipulation and projective readout⁸ were demonstrated.

The purpose of entangled qubit pairs is to convey quantum information through a computing device.¹ The entanglement of two spin qubits may be uniquely defined through von Neuman entropy or, equivalently, concurrence.^{9,10} A pair of qubits may be realized, e.g., as two separate regions, each occupied by one electron in a state $|s\rangle_{A,B}$ of either spin, $s = \uparrow$ or \downarrow . For a system in a pure state $|\Psi_{AB}\rangle = \sum_{ss'} \alpha_{ss'} |s\rangle_A \otimes |s'\rangle_B$, the concurrence as a quantitative measure for (spin) entanglement is given by¹⁰ $C_0 = 2|\alpha_{\uparrow\downarrow}\alpha_{\downarrow\uparrow} - \alpha_{\uparrow\uparrow}\alpha_{\downarrow\downarrow}|$. Two qubits are completely entangled, $C_0 = 1$, if they are in one of the Bell states⁹—e.g., singlet $|\Psi_{AB}\rangle \propto |\uparrow\downarrow\rangle - |\downarrow\uparrow\rangle$.

The setup and main results. We focus on entanglement between two electrons confined in two adjacent quantum dots weakly coupled by electron tunneling in a controllable manner, Fig. 1(a). The interdot tunneling matrix element t determines not only the tunneling rate, but also the effective magnetic superexchange interaction $J \sim 4t^2/U$, where U is the scale of Coulomb interaction between two electrons confined on the same dot. By adjusting a global back-gate voltage, exactly two electrons can be confined to the dots A and B on average.

Additional gate voltages are applied to independently control tunneling to the electrodes, t_n . Depending on the values of t_n , various topologies can be realized, and even for very weak coupling, the spin of confined electrons may be screened due to the Kondo effect, where at temperatures be-

low the Kondo temperature T_K a spin-singlet state is formed between a confined electron and conduction electrons close to the Fermi energy. Conductance and some other properties of such systems have already been studied, without considering, however, an analysis of entanglement and its relationship to the many-body phenomena embodied in the Kondo effect.

Qualitatively the physics related to qubit pairs in coupled DQD's can be summarized as follows.

(i) If t/U is not small, the electrons tunnel between the dots and charge fluctuations introduce additional states with zero or double occupancy of individual dots.^{11,12} Due to significant local charge fluctuations, this regime is not particularly appropriate for the spin-qubit manipulation.

(ii) For systems with strong electron-electron repulsion, charge fluctuations are suppressed and the states with single occupancy—the spin qubits—dominate. Due to the effective antiferromagnetic Heisenberg interaction, the spins A and B tend to form a singlet state. The physics of such qubit pairs may be compared to the two-impurity Kondo problem studied by Jones, Varma, and Wilkins two decades ago.¹³ There

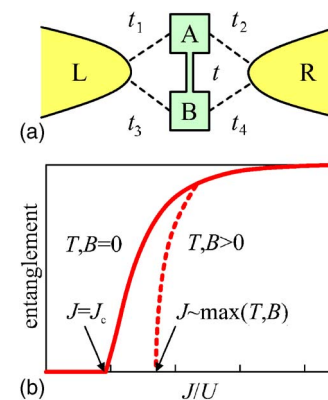


FIG. 1. (Color online) (a) Double-quantum-dot system. t and t_n are the matrix elements for tunneling between dots A and B and from the dots to the electrodes, respectively. (b) Entanglement between two spins on the quantum dots as a function of the interdot exchange coupling J : below J_c , the two spins are not entangled and the DQD is in some type of the Kondo regime. For elevated temperatures and magnetic field above J_c , the entanglement is zero if $J \lesssim \max(T, B)$.

two impurities form either two Kondo singlets with delocalized electrons or bind into a local spin-singlet state that is virtually decoupled from delocalized electrons. The crossover between the two regimes is determined by the relative values of the exchange energy J and twice the Kondo condensation energy, of order of the Kondo temperature T_K .

As shown in this paper, our numerical results for representative DQD systems with different topologies of possible experimental realizations reveal much more diverse physical behavior. However, (i) in all cases the spin qubits are unentangled for J below some critical value J_c , where the actual value of J_c crucially depends on the setup topology, and (ii) at elevated temperatures $T > 0$ and external magnetic field $B \neq 0$ the entanglement is additionally suppressed and generically zero when $J \leq \max(J_c, T, B)$, as schematically shown in Fig. 1(b).

Quantitative results. For simplicity we model DQD using the two-site Hubbard Hamiltonian $H = -t \sum_s (c_{A_s}^\dagger c_{B_s} + c_{B_s}^\dagger c_{A_s}) + U \sum_{i=A,B} n_{i\uparrow} n_{i\downarrow}$, where $c_{i_s}^\dagger$ creates an electron with spin s in the dot $i=A$ or $i=B$ and $n_{i_s} = c_{i_s}^\dagger c_{i_s}$ is the number operator. Interdot repulsion is neglected here because significant effects are found only in the regime of interdot charging energy comparable with on-site repulsion U .¹⁸ There the SU(4) spin-isospin description is more appropriate in comparison with the spin-qubit pairs picture investigated here. The dots are coupled to the left and right noninteracting lead as shown in Fig. 1(a).

DQD's as considered here cannot be described with a pure quantum state, and concurrence is not directly given by C_0 . It is related to the reduced density matrix of the DQD subsystem,^{10,14,15} where for systems that are axially symmetric in spin space the concurrence may conveniently be given in the closed form¹⁶

$$C = \max(0, C_{\uparrow\downarrow}, C_{\parallel}) / (P_{\uparrow\downarrow} + P_{\parallel}),$$

$$C_{\uparrow\downarrow} = 2|\langle S_A^+ S_B^- \rangle| - 2\sqrt{\langle P_A^\uparrow P_B^\uparrow \rangle \langle P_A^\downarrow P_B^\downarrow \rangle},$$

$$C_{\parallel} = 2|\langle S_A^+ S_B^+ \rangle| - 2\sqrt{\langle P_A^\uparrow P_B^\downarrow \rangle \langle P_A^\downarrow P_B^\uparrow \rangle}, \quad (1)$$

where $S_i^\pm = (S_i^z)^\pm = c_{i\uparrow}^\dagger c_{i\downarrow}$ is the electron spin raising operator for dot $i=A$ or B and $P_i^s = n_{i_s} (1 - n_{i,-s})$ is the projection operator onto the subspace where dot i is occupied by one electron with spin s . $P_{\uparrow\downarrow} = \langle P_A^\uparrow P_B^\downarrow + P_A^\downarrow P_B^\uparrow \rangle$ and $P_{\parallel} = \langle P_A^\uparrow P_B^\uparrow + P_A^\downarrow P_B^\downarrow \rangle$ are probabilities for antiparallel and parallel spin alignment, respectively.

We have determined concurrence for all three possible topologically nonequivalent two-terminal experimental arrangements: double quantum dots (i) coupled in series, (ii) laterally side coupled, and (iii) coupled in parallel. Concurrence was determined numerically from Eq. (1), where expectation values correspond to a many-body state with the chemical potential in the middle of the electron band, which guarantees that the dots are singly occupied, $\langle n_{A,B} \rangle = 1$. Our extensive investigation over the full parameter range for various topologies indicates that all show generic behavior outlined in Fig. 1(b), but quantitatively can differ by many orders of magnitude, which should be taken into consideration in experiments with such DQD's. Numerical methods

were based on the Gunnarsson-Schönhammer (GS) projection-operator¹⁷⁻¹⁹ and numerical renormalization group²⁰⁻²² (NRG) methods.

Serially coupled DQD's. First we consider serially coupled DQD's, which model entangled pairs that may be extracted using a single-electron turnstile.²³ Here $t_{1,4} = t'$ and $t_{2,3} = 0$ with the hybridization width of each dot $\Gamma = (t')^2/t_0$, where $4t_0$ is the bandwidth of noninteracting leads. Entanglement of a qubit pair represented by quantum dots in contact with the leads (fermionic bath) was not quantitatively determined so far, although this system has already been extensively studied (Refs. 18, 24, and 25 and references therein).

In analogy with entanglement at zero temperature studied recently in a many-body ground state,²⁶ we consider here the concurrence of DQD's at fixed temperature and static magnetic field along the z -axis. Expectation values $\langle \dots \rangle$ in the concurrence formula (1) correspond to thermal equilibrium of the system; therefore, $\langle S_A^+ S_B^+ \rangle = 0$ here. Qualitatively, the concurrence is significant when enhanced spin-spin correlations indicate interdot singlet formation. As shown in Fig. 2, the correlator $\langle S_A \cdot S_B \rangle$ tends to $-3/4$ for J large enough to suppress the formation of Kondo singlets, but still $J/U \ll 1$, that local charge fluctuations Δn_A^2 are sufficiently suppressed and $P_{\uparrow\downarrow} + P_{\parallel} \rightarrow 1$. Concurrence, calculated for various values of the Coulomb interaction strengths and in the absence of magnetic field, is presented in Fig. 2, left bottom panel. As discussed above, C is zero for $J < J_{1c}$ due to the Kondo effect, which leads to entanglement between localized and conducting electrons²⁷ instead of the A-B qubit pair entanglement. In finite magnetic field irrespective of temperature the concurrence abruptly tends to zero for $B > J$ (not shown here).²⁸

In particular, the local dot-dot singlet is formed and $C \geq 0$ whenever singlet-triplet splitting $J > J_{1c} \sim 2.5T_K(\Gamma)$, where the Kondo temperature is given by the Haldane formula $T_K(\Gamma) = \sqrt{U\Gamma}/2 \exp(-\pi U/8\Gamma)$. This is presented in the phase diagram in the $(U/\Gamma, J/T_K)$ plane, Fig. 3. The dashed region corresponds to the regime of zero concurrence and is delimited by the line of the critical $J = J_{1c}$ (red line). The charge fluctuations (Fig. 3, contour plot) are suppressed for sufficiently large repulsion—i.e., $U/\Gamma \geq 10$. In this limit and in vanishing magnetic field, the DQD can be described in terms of the Werner states²⁹ and becomes similar to recently studied problem of entanglement of two Kondo spin impurities embedded in a conduction band.³⁰ In this case, $C_{\uparrow\downarrow} \sim 2(-\langle S_A \cdot S_B \rangle - \frac{1}{4}) \sim P_{\uparrow\downarrow} - 2P_{\parallel}$ for $C_{\uparrow\downarrow} \geq 0$. For large U/Γ , where the charge fluctuations vanish, the $\langle S_A \cdot S_B \rangle = -\frac{1}{4}$ boundary (Fig. 3, dotted line) progressively merges with the $C=0$ line.

Side-coupled DQD. In the side-coupled DQD configuration $t_{1,2} = t'$, $t_{3,4} = 0$ (Fig. 2, middle), dot A is in direct contact with the electrodes, while dot B couples to the conduction band only indirectly through dot A. Because the two electrodes are in contact only with dot A, $\Gamma = 2(t')^2/t_0$ —i.e., twice as much as in the previous case. Since $T_K \propto \exp(-\pi U/8\Gamma)$, the Kondo temperature on dot A is strongly enhanced.

For $J > J_{2c}$, the spins bind in an antiferromagnetic singlet, as in all other cases. For $J < J_{2c}$, the system enters the “two-

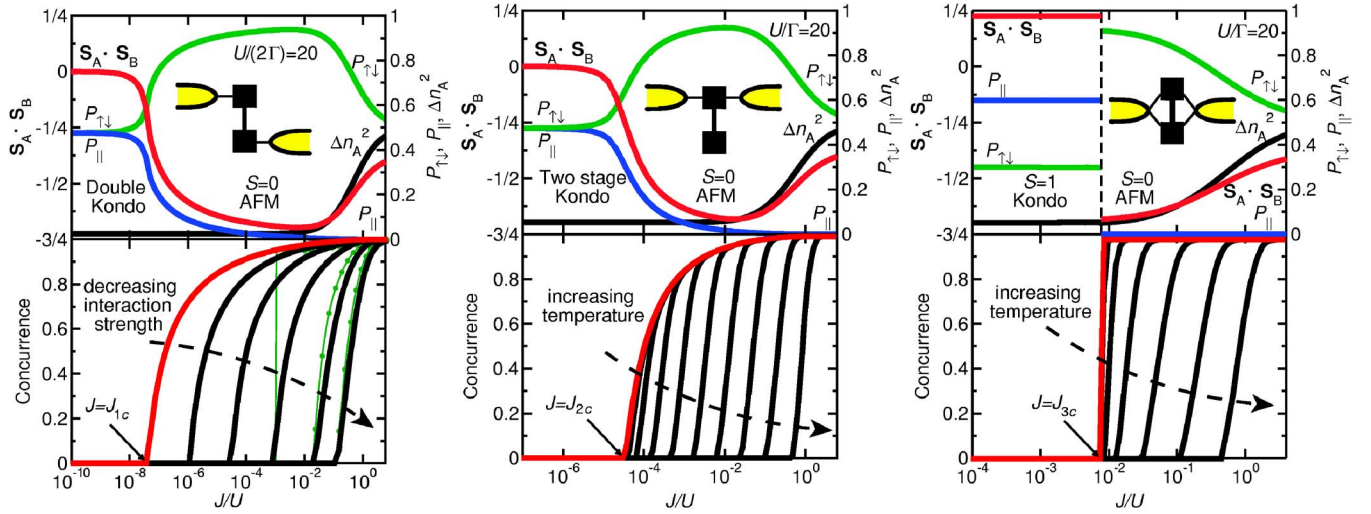


FIG. 2. (Color online) *Top panels:* spin-spin correlation function $S_A \cdot S_B$, charge fluctuations on one quantum dot, Δn_A^2 , and probabilities $P_{\uparrow\downarrow}$, P_{\parallel} for $T \ll T_K$, $B \rightarrow 0$ and with $t' = t_0/\sqrt{20}$. *Bottom left panel:* concurrence C , corresponding to serially coupled dots, for a range of interactions $U/\Gamma = 40, 32, 24, 16, 8, 4$ and calculated with both the NRG and GS methods (bullets), yielding the same J_{1c} , but due to the limited span of variational basis the GS method progressively overestimates C for $U/\Gamma \gtrsim 20$ regime. *Bottom right two panels:* the results for side-coupled and parallel configurations obtained from the NRG method. Temperatures range from the scale of the Coulomb repulsion parameter U , $T/U = 0.4$, to temperatures below the Kondo scale T_K ; each consecutive curve corresponds to a temperature lowered by a factor of 4.

stage Kondo" regime, characterized by consecutive screening of local moments.^{21,31,32} At the Kondo temperature $T_K^{(1)} = T_K(\Gamma)$ the spin on dot A is screened, while the spin on dot B is compensated for at a reduced temperature

$$T_K^{(2)} = d_1 T_K^{(1)} \exp(d_2 J/T_K^{(1)}), \quad (2)$$

where $d_{1,2}$ are constants of order unity. The Kondo effect on dot A leads to the formation of a local Fermi liquid for temperatures below $T_K^{(1)}$. The quasiparticle excitations of this Fermi liquid then participate in the Kondo effect on dot B at much lower Kondo temperature $T_K^{(2)}$.³¹ Such a description is valid only when the temperature scales $T_K^{(1)}$ and $T_K^{(2)}$ are widely separated. This no longer holds when J becomes comparable to $T_K^{(1)}$; see Eq. (2). The critical J_{2c} is thus still given by $J_{2c} \sim T_K^{(1)}$. The crossover is very smooth, and the

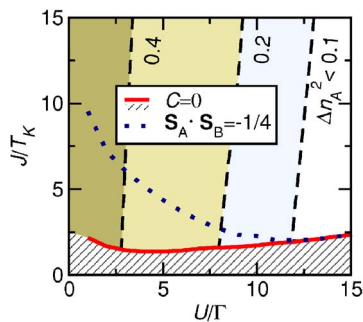


FIG. 3. (Color online) In the phase diagram $(U/\Gamma, J/T_K)$ a solid line separates $C > 0$ and $C = 0$ regions (line shaded), together with dotted line indicating $\langle S_A \cdot S_B \rangle = -1/4$ ($T \rightarrow 0$ and $B = 0$). Both lines merge for $U/\Gamma \gtrsim 12$, where charge fluctuations Δn_A^2 progressively become negligible (contour plot).

transition from the interimpurity singlet phase to the Kondo phase does not exhibit any sharp features. In fact, the low-temperature fixed point is the same for $J < J_{2c}$ and $J > J_{2c}$, unlike in the case of DQD's in series. In the latter case, the Kondo phase and the interimpurity singlet phase are qualitatively different and are characterized by different electron scattering phase shifts.

In the $J > J_{2c}$ singlet region, when the temperature is above J , the exchange interaction is too weak to bind the spins into a singlet and the entanglement is lost (see Fig. 2, bottom middle panel). In the $J < J_{2c}$ Kondo region, the concurrence is zero irrespective of temperature: for $T < T_K$ it is zero due to the Kondo effect, and for $T > T_K$ the spin-singlet cannot be restored, since $T > J$. The elevated temperature and magnetic field dependence is similar to the previous case of serially coupled dots.²⁸

Parallely coupled DQD's. In the case of parallel quantum dots [$t_n \equiv t'$ and $\Gamma = 2(t')^2/t_0$] the physics is markedly different from the case of the previous two configurations. The conduction band mediated effective Ruderman-Kittel-Kasuya-Yoshida (RKKY) interaction between the dots is, in our simplified model, ferromagnetic.²² Here the spins order ferromagnetically into a triplet state (Fig. 2, right panels) and undergo a $S = 1$ Kondo screening at low temperatures in the regime

$$J < |J_{\text{RKKY}}| \sim c \frac{64 \Gamma^2}{\pi^2 U}, \quad (3)$$

where c is a constant of order unity. This yields an uncompensated $S = 1/2$ residual spin, and since half a unit of spin is quenched by the conduction band via the Kondo effect, there clearly cannot be any entanglement between the electrons on the dots. For $J > |J_{\text{RKKY}}|$, the antiferromagnetic ordering wins

and, once again, the electrons form an entangled singlet state. The transition from the Kondo phase to the singlet phase is in this case a true quantum phase transition,²² and the concurrence drops abruptly from (surprisingly) $C \approx 1$ to $C=0$ when the exchange J between the dots is decreased below some J_{3c} . Critical coupling J_{3c} is not determined by T_K , as previously, but rather by $|J_{\text{RKKY}}|$. For this reason, concurrence drops to zero at a much higher temperature (compare the middle and right bottom panels in Fig. 2) and is strictly zero for $J \lesssim T$ as in the previous two cases. In finite magnetic field $C=0$ if $J \lesssim |J_{\text{RKKY}}| + B$ (not shown here).²⁸

If the couplings t_n are not strictly equal, another Kondo screening stage may occur at low temperatures, in which the residual $S=1/2$ spin is finally screened to zero.³³ In this case the quantum phase transition is replaced by a crossover that becomes smoother as the degree of asymmetry between the couplings t_n increases (results not shown).

Conclusions. We have found generic behavior of spin-entanglement of an electron pair in double quantum dots. On the one hand, we have shown quantitatively that making the spin-spin exchange coupling J large by increasing tunneling t leads to enhanced charge fluctuations, while on the other, a small interaction $J < J_c$ suppresses entanglement as the DQD system undergoes some form of the Kondo effect. Various

regimes are explained analytically and supported with typical numerical examples. In the limiting cases we found (i) two separate Kondo effects for serially coupled DQD, (ii) two-stage Kondo effect in side-coupled DQD, and (iii) $S=1$ Kondo effect with underscreening for parallel-coupled DQD's, eventually followed by another $S=1/2$ Kondo effect at lower temperatures. For two terminal setups, these are the only possible types of the Kondo effect; in a generic situation with arbitrary t_n , one of these possibilities must occur.

In all cases, in spite of different Kondo mechanisms, the temperature and magnetic field dependence of entanglement is proven to be determined solely by the exchange scale J and not by the much lower scale of the Kondo temperature, which explains the universal behavior of the entanglement shown in Fig. 1(b). Critical J_c , however, will for various experimental setups vary for several orders of magnitude.

We thank I. Sega for inspiring discussions and J. H. Jefferson for valuable comments regarding the manuscript. We thank T. Rejec for his GS code. One of the authors (A.R.) acknowledges a helpful discussion with R. H. McKenzie. We acknowledge support from the Slovenian Research Agency under Contract No. PI-0044.

-
- ¹M. A. Nielsen and I. L. Chuang, *Quantum Computation and Quantum Information* (Cambridge University Press, Cambridge, England, 2000).
- ²D. Loss and D. P. DiVincenzo, Phys. Rev. A **57**, 120 (1998).
- ³D. P. DiVincenzo, Science **270**, 255 (1995).
- ⁴W. A. Coish and D. Loss, cond-mat/0603444 (unpublished).
- ⁵J. M. Elzerman, R. Hanson, J. S. Greidanus, L. H. Willems van Beveren, S. D. Franceschi, L. M. K. Vandersypen, S. Tarucha, and L. P. Kouwenhoven, Phys. Rev. B **67**, 161308(R) (2003).
- ⁶J. C. Chen, A. M. Chang, and M. R. Melloch, Phys. Rev. Lett. **92**, 176801 (2004).
- ⁷T. Hatano, M. Stopa, and S. Tarucha, Science **309**, 268 (2005).
- ⁸J. R. Petta, A. C. Johnson, J. M. Taylor, E. A. Laird, A. Yacoby, M. D. Lukin, C. M. Marcus, M. P. Hanson, and A. C. Gossard, Science **309**, 2180 (2005).
- ⁹C. H. Bennett, H. J. Bernstein, S. Popescu, and B. Schumacher, Phys. Rev. A **53**, 2046 (1996).
- ¹⁰W. K. Wootters, Phys. Rev. Lett. **80**, 2245 (1998).
- ¹¹J. Schliemann, D. Loss, and A. H. MacDonald, Phys. Rev. B **63**, 085311 (2001).
- ¹²P. Zanardi, Phys. Rev. A **65**, 042101 (2002).
- ¹³B. A. Jones, C. M. Varma, and J. W. Wilkins, Phys. Rev. Lett. **61**, 125 (1988).
- ¹⁴A. Osterloh, L. Amico, G. Falci, and R. Fazio, Nature (London) **416**, 608 (2002).
- ¹⁵O. F. Syljuåsen, Phys. Rev. A **68**, 060301(R) (2003).
- ¹⁶A. Ramšak, I. Sega, and J. H. Jefferson, Phys. Rev. A **74**, 010304(R) (2006).
- ¹⁷K. Schönhammer and O. Gunnarsson, Phys. Rev. B **30**, 3141 (1984).
- ¹⁸J. Mravlje, A. Ramšak, and T. Rejec, Phys. Rev. B **73**, 241305(R) (2006).
- ¹⁹T. Rejec and A. Ramšak, Phys. Rev. B **68**, 035342 (2003).
- ²⁰H. R. Krishna-murthy, J. W. Wilkins, and K. G. Wilson, Phys. Rev. B **21**, 1003 (1980).
- ²¹R. Žitko and J. Bonča, Phys. Rev. B **73**, 035332 (2006).
- ²²R. Žitko and J. Bonča, Phys. Rev. B **74**, 045312 (2006).
- ²³X. Hu and S. DasSarma, Phys. Rev. B **69**, 115312 (2004).
- ²⁴A. Georges and Y. Meir, Phys. Rev. Lett. **82**, 3508 (1999).
- ²⁵W. Izumida and O. Sakai, Phys. Rev. B **62**, 10260 (2000).
- ²⁶A. N. Jordan and M. Büttiker, Phys. Rev. Lett. **92**, 247901 (2004).
- ²⁷A. Rycerz, Eur. Phys. J. B **52**, 291 (2006); S. Oh and J. Kim, Phys. Rev. B **73**, 052407 (2006).
- ²⁸R. Žitko, J. Bonča, and A. Ramšak (unpublished).
- ²⁹R. F. Werner, Phys. Rev. A **40**, 4277 (1989).
- ³⁰S. Y. Cho and R. H. McKenzie, Phys. Rev. A **73**, 012109 (2006).
- ³¹P. S. Cornaglia and D. R. Grempel, Phys. Rev. B **71**, 075305 (2005).
- ³²M. Vojta, R. Bulla, and W. Hofstetter, Phys. Rev. B **65**, 140405(R) (2002).
- ³³C. Jayaprakash, H. R. Krishna-murthy, and J. W. Wilkins, Phys. Rev. Lett. **47**, 737 (1981).